Erschienen in: ChemBioChem ; 18 (2017), 23. - S. 2312-2316
https://dx.doi.org/10.1002/cbic.201700355

Simultaneous IR-Spectroscopic Observation of α-Synuclein, Lipids, and Solvent Reveals an Alternative Membrane-Induced Oligomerization Pathway

Mohammad A. Fallah,[a] Hanne R. Gerding,[b] Christian Scheibe,[a] Malte Drescher,[a] Christiaan Karreman,[b] Stefan Schildknecht,[b] Marcel Leist,[b] and Karin Hauser*[a]

The intrinsically disordered protein α-synuclein (αS), a known pathogenic factor for Parkinson's disease, can adopt defined secondary structures when interacting with membranes or during fibrillation. The αS–lipid interaction and the implications of this process for aggregation and damage to membranes are still poorly understood. Therefore, we established a label-free infrared (IR) spectroscopic approach to allow simultaneous monitoring of αS conformation and membrane integrity. IR showed its unique sensitivity for identifying distinct β-structured aggregates. A comparative study of wild-type αS and the naturally occurring splicing variant αS Δexon3 yielded new insights into the membrane's capability for altering aggregation pathways.

The 140-amino-acid protein α-synuclein (αS) is the major component of the cytoplasmic protein aggregates (Lewy bodies) found in the brains of patients suffering from Parkinson's disease (PD).[1] Strong genetic evidence links αS with human disease pathogenesis.[2] Although monomeric αS is classified as a soluble and intrinsically disordered protein (IDP), it is known to form various types of aggregates once a critical concentration is exceeded.[3] There is also substantial evidence that αS directly interacts with lipids and membranes[4] and that membrane binding is crucial for the biological function of αS.[5] Upon interaction with lipid membranes, the N-terminal region of αS forms α-helices with one axis parallel to the lipid surface and with one half of the helix embedded in the lipid layer.[6] Lipids have been found within Lewy bodies, so it is likely that the interaction of lipids with αS is relevant for aggregation.[7] Oligomers of αS can also form membrane pores,[8] and microscopy studies suggest that aggregated αS compromises membrane integrity.[7]

To elucidate the correlation between the αS aggregation process and membrane interaction, we developed an infrared (IR) spectroscopic approach for simultaneous monitoring of αS conformational changes and membrane integrity without the need to introduce additional probes for detection. IR spectroscopy has previously been used to study fibrillation and amyloid formation of proteins.[9] This method is particularly well suited to detect subtle structural changes.[10] The IR marker band commonly used for secondary structure analysis of proteins is the amide I band (mainly C=O stretching vibration of the polypeptide backbone). Band deconvolution into subcomponents can yield an estimate of contributing fractions of secondary structure elements (disordered, α-helix, β-sheet) and different forms of β-structured aggregates, although interpretation has to be done carefully.[11] Selected vibrational modes of the lipids (head groups, carbonyl ester, alkyl chains) can likewise be used as chemical reporters for the interaction between αS and the membrane. Furthermore, vibrational modes of water can be consulted because they change when larger membrane disruptions cause water displacement.

We utilized attenuated total reflection Fourier-transform infrared (ATR-FTIR) difference spectroscopy to study interactions of αS wild type (wt) and of the splicing variant αS Δexon3 with solid-supported lipid bilayers (SSLBs) used as biomimetic membranes. αS Δexon3 lacks the amino acids 41–54 of αS wt. Although this variant is naturally expressed in humans, information on its conformational behavior is scarce.[12] As a monomer, αS Δexon3 is an IDP, but the propensity to form helical secondary structures upon membrane interaction is expected to be altered in this αS variant. The comparison of two molecularly relatively similar variants of a disease-relevant protein appeared to be an interesting challenge both to test the performance of this method and to fill the knowledge gap on αS Δexon3.

Initially, conformational changes and aggregation of the two αS variants in the absence of a membrane were assessed (Figure 1). The amide I spectra ($t = 10$ min, blue) indicate an intrinsically disordered state in solution for both variants, with some residual structures.[6c,13] A slow aggregation process is observed over time, but with striking differences: αS wt reveals two bands at 1665 and 1618 cm^{-1} whereas αS Δexon3 exhibits a broad band with a maximum at 1630 cm^{-1} ($t = 24$ h, red). Protein sedimentation in the evanescent field of the IR probe beam explains the increased band intensities over time. To resolve the conformational heterogeneity qualitatively, band deconvolution was performed (for details see Figures S1 and S2 in the Supporting Information). The band at 1665 cm^{-1} is assigned to various structural elements (β-turns, loops, and helices) that all absorb in this frequency range.[14] Native β-sheets in proteins absorb in the 1630–1640 cm^{-1} range, whereas

[a] Dr. M. A. Fallah, C. Scheibe, Prof. Dr. M. Drescher, Prof. Dr. K. Hauser
Department of Chemistry, University of Konstanz
Universitätsstrasse 10, 78457 Konstanz (Germany)
E-mail: karin.hauser@uni-konstanz.de

[b] H. R. Gerding, Dr. C. Karreman, Dr. S. Schildknecht, Prof. Dr. M. Leist
Department of Biology, University of Konstanz
Universitätsstrasse 10, 78457 Konstanz (Germany)

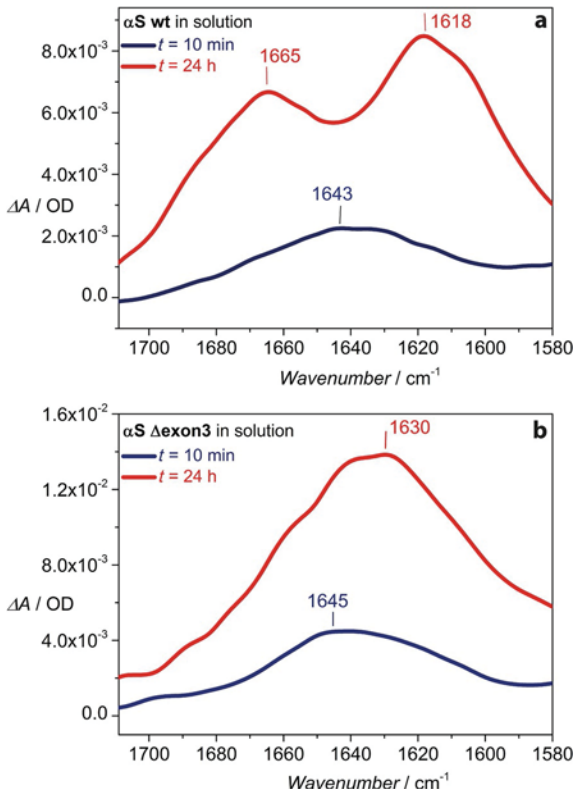

Figure 1. Aggregate formation in solution: A) wt, and B) αS Δexon3. The disordered structure (blue, 10 min) aggregated over time. The two variants developed different aggregate species (red, 24 h).

β-structured aggregates typically absorb below 1630 cm^{-1}. A very low frequency indicates a well-ordered extended β-sheet (fibril) with strong hydrogen bonds formed between the backbone amide carbonyl groups along the fibril axis. An additional (weak) band absorbing in the 1685–1695 cm^{-1} range gives evidence of antiparallel β-structure.[9b–d] Both variants reveal heterogeneity of β-structured aggregates, but with a different distribution as indicated by the amide I band shape and deconvolved components (Figure S2). We propose that the aggregate structures include extended fibrils and less-fibrillar, more compact oligomers as schematically illustrated in Figure 5 A, B (below): the fibrillar aggregates dominate in αS wt and the oligomers prevail in αS Δexon3. Thus, aggregation in solution is characterized by a slow process that is substantially different for each of the variants.

Membranes are known to induce αS aggregation, but detailed interaction mechanisms are still unclear. In this study, we compared conformational changes in two αS variants evoked by the presence of a membrane and examined the functional role of the membrane in the aggregation process. The sensitivity of our IR approach is ideally suited because it resolves the formation of various aggregates in a time-dependent manner and further detects the membrane. We prepared a SSLB of 1-palmitoyl-2-oleoyl-*sn*-glycero-3-phosphocholine (POPC) and 1-palmitoyl-2-oleoyl-*sn*-glycero-3-phospho-*rac*-glycerol (POPG; 1:1) as model membrane on the internal reflection element (IRE) of the ATR cell. POPC bilayer formation on an IRE has been reported before,[15] and it is known that αS binds to acidic phospholipids such as POPG. Other lipids as GM1 gangliosides and cholesterol also interact specifically with αS and amyloid peptides.[16] Mechanisms of ganglioside/cholesterol-dependent amyloid pore formation were suggested, but inhibition of αS fibrillation by GM1 interaction was also observed.[17] The POPC/POPG model membrane used here facilitates both αS binding and fibrillation.

We monitored the bilayer formation through IR difference spectra (Figure S3). It remained stable over several hours (> 12 h), and even rigorous rinsing did not compromise the integrity of the bare SSLB. Furthermore, polarized ATR-FTIR spectra confirmed the long-term stability of the SSLB (Figure S4).

Whereas in the absence of the membrane, an intrinsically disordered state in both αS variants prevailed after 10 min (Figure 1, blue), the presence of the membrane resulted in a shift of the amide I band maximum towards ≈1650 cm^{-1} and changed the band shape (Figure S5). Band deconvolution revealed conformational heterogeneity upon short-term membrane interaction. In agreement with results of other studies that found that the N-terminal region of αS preferentially adopts an α-helical structure upon membrane binding,[13,18] we also detected α-helical conformation as the dominant secondary structure in both αS variants. Interestingly, the shorter N-terminal region of αS Δexon3 (lack of amino acids 41–54) did not prevent α-helix formation upon membrane interaction. IR spectroscopy furthermore revealed that β-aggregates had already developed in the early stages of membrane interaction and that the membrane significantly accelerated the aggregation process. The detection of coexisting conformations highlights the sensitivity of this method.

Conformational changes in αS wt and αS Δexon3 at the membrane–solvent interface were detected after an 8 h incubation period (Figure 2). Long-term conformational changes are governed not only by direct membrane contact, but also by protein–protein interactions. In contrast with the aggregation observed in solution (Figure 1), the similar amide I band shapes indicated almost identical distributions of secondary structures and aggregates for both αS variants. Hence, our IR experiments revealed that the membrane mechanistically changed the oligomerization pathway, and this effect was particularly obvious for αS wt. Therefore, we attribute an important function in the aggregation mechanism of αS to the membrane. To assess kinetic properties, the growth of aggregate species at 1626 cm^{-1} was recorded over 8 h (Figure 3). Significantly faster aggregation was observed for αS Δexon3 than for αS wt. We assume that this implies a longer membrane interaction with temporary intermediate structures for αS wt.

We finally concentrated on membrane integrity to determine whether it is the accumulation of certain aggregate species or the process of aggregation that is critical for membrane damage (Figure 4). The lipid bands were slightly frequency-shifted in relation to the pure SSLB spectrum (Figure S3) and showed positive and negative intensities. Negative lipid bands indicate perturbation of the lipid molecules whereas positive lipid bands might be caused by lipidated proteins.[15b] This agrees with other studies that suggested that interaction with

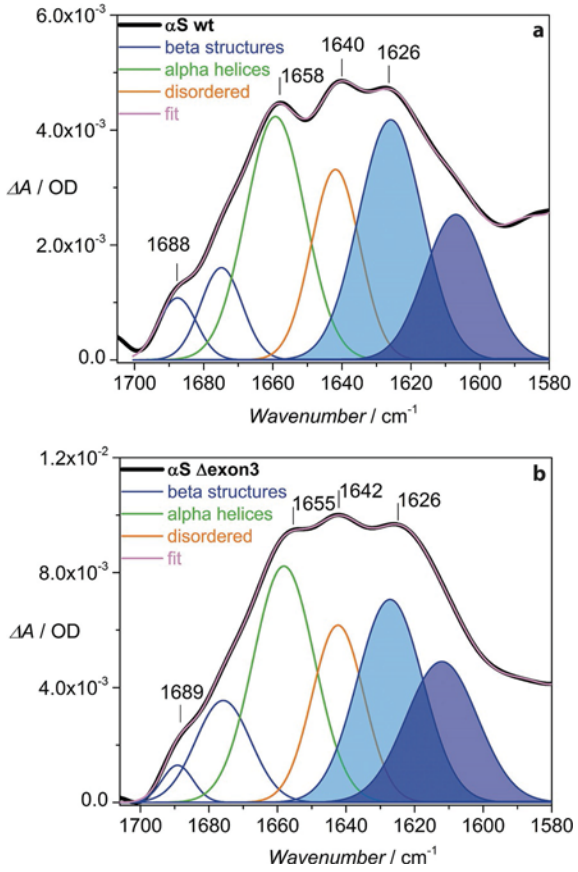

Figure 2. Conformational changes in A) αS wt, and B) αS Δexon3 after long-term membrane interaction (8 h). Band deconvolution revealed similar distributions of structural states, in particular of β-structured aggregates ($< 1630\ cm^{-1}$), for the two isoforms, in contrast to aggregation in solution. The membrane thus induced a mechanistic change in the aggregation process.

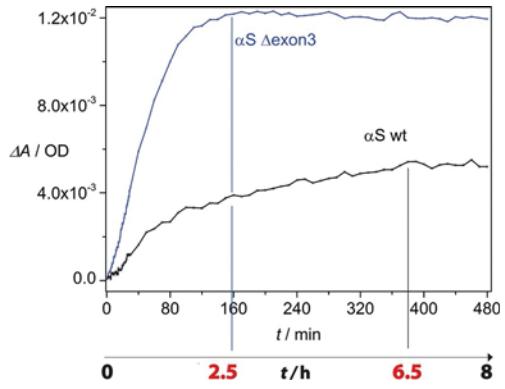

Figure 3. Different kinetics of aggregate growth for αS wt and αS Δexon3. The aggregate species monitored at ≈1626 cm^{-1} form much more rapidly and to a larger extent in the case of αS Δexon3.

amyloid proteins can cause membrane remodeling through lipid extraction, protein lipidation, and lipid clustering.[19] Thus, analysis of the lipid bands hinted at a complex interaction mechanism involving protein lipidation and membrane perturbation.

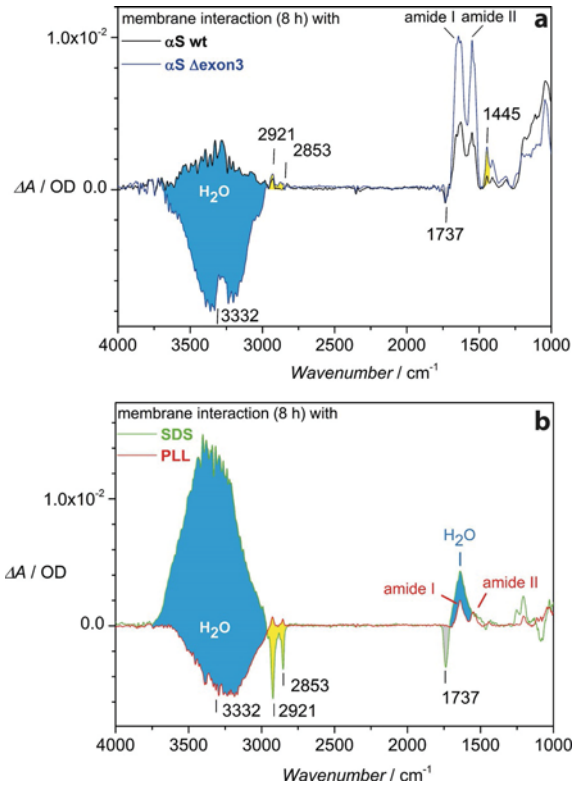

Figure 4. Membrane integrity monitored through lipid and water bands. A) αS wt (black) and αS Δexon3 (blue). B) SDS (green) and PLL (red) as control measurements.

To quantify membrane integrity further, we used the O–H stretching mode of water at ≈3330 cm^{-1} as a vibrational reporter (Figure S6). Protein sedimentation onto the SSLB surface displaces water molecules, resulting in a negative water band. Positive water bands are indicative of membrane disruption because the membrane disruption is followed by the appearance of an increased number of water molecules in the vicinity of the IRE. These opposite spectral effects are illustrated in our control experiments with poly-L-lysine (PLL) for protein sedimentation and with sodium dodecyl sulfate (SDS) for membrane disruption (Figure 4B). When PLL sedimented on the SSLB (as indicated by the rise of amide I and amide II bands), the negative water band revealed the displacement of water by PLL. SDS disrupts membranes thoroughly, and we observed positive water bands (and negative lipid bands). Both αS variants aggregated upon membrane interaction, consequently displacing water from the SSLB surface. This explains the negative water bands observed for αS Δexon3 (Figure 4A). However, interaction between αS wt and the SSLB led to a slight, but reproducible, positive water band at 3330 cm^{-1}. This implies that the negative water absorbance was slightly compensated for by the positive water band, and significant disturbance of membrane integrity was thus observed for αS wt.

Because the conformational heterogeneity was almost the same for both αS variants (Figure 2), it is unlikely that a particular aggregate species was responsible for the substantial membrane damage. The aggregates settle on the membrane

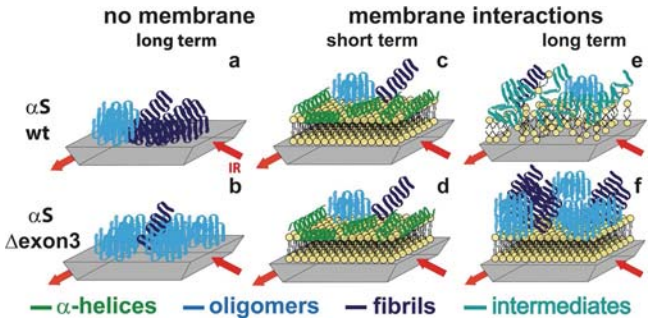

Figure 5. Schematic summary of ATR-FTIR experiments with new hypothesis about aggregation pathways. Aggregation in solution is slow and characterized by a different distribution of β-structured aggregates for A) αS wt, and B) αS Δexon3. The membrane significantly accelerates aggregation and changes the oligomerization pathway. C), D) Both variants adopt an α-helical structure (green) upon membrane binding accompanied by the formation of various β-structured aggregates (short-term interactions). A similar aggregate distribution is observed after long-term interactions, but aggregate formation occurs with different kinetics. E) Membrane disruption is detected for αS wt, but F) no significant membrane damage is seen in the case of αS Δexon3, due to different aggregate–membrane interactions.

without disturbing it appreciably, as observed for αS Δexon3 (Figure 4A and Figure 5F). A striking difference between the aggregation kinetics of the two variants was found, and the presence of the membrane changed the aggregation mechanism significantly, especially in the case of αS wt. We thus attribute membrane disruption mainly to intermediate states of αS wt that interact with the membrane (Figure 5E). Although we could not resolve distinct intermediate states, it is likely that the N-terminal region is important in the formation of intermediates that affect membrane integrity.

In summary, we have developed an ATR-FTIR spectroscopic approach and demonstrated its high sensitivity for simultaneously studying protein aggregation mechanisms and membrane interaction. The combined analysis of protein, lipid, and water vibrational modes, reported here for the first time, allows the differentiation of distinct aggregate species, to evaluate aggregation kinetics and to assess membrane integrity on a molecular level. We analyzed two αS variants (αS wt and αS Δexon3) that formed different β-structured aggregate species in solution. The aggregation process was significantly accelerated by the presence of a membrane, but, most notably, the membrane changed the mechanism from the process observed in solution. The heterogeneous distributions of the β-structured aggregates were quite similar for the two variants, although the aggregates evolved with different kinetics. We detected differences in membrane integrity, and we assume that it is not the final aggregates, but rather the aggregation pathway and interaction with intermediates, that are crucial for membrane remodeling and disruption. We obtained the first clue that modulations in the ratio of endogenously formed αS wt and the naturally occurring splice variant αS Δexon3 might affect the (patho)physiological properties of the Parkinson's-associated protein αS in cells.

Acknowledgements

This work was supported by the Deutsche Forschungsgemeinschaft (SFB 969 and SFB 1214) and the Konstanz Research School Chemical Biology. We gratefully acknowledge fruitful discussions with Vinod Subramaniam and Christine Peter.

Conflict of Interest

The authors declare no conflict of interest.

Keywords: aggregation · alpha-synuclein · ATR-FTIR · protein–membrane interaction · solid-supported lipid bilayers

[1] M. G. Spillantini, M. L. Schmidt, V. M. Y. Lee, J. Q. Trojanowski, R. Jakes, M. Goedert, *Nature* **1997**, *388*, 839–840.

[2] a) M. H. Polymeropoulos, C. Lavedan, R. L. Nussbaum, *Science* **1997**, *276*, 2045–2047; b) V. M. Nemani, W. Lu, V. Berge, K. Nakamura, B. Onoa, M. K. Lee, F. A. Chaudhry, R. A. Nicoll, R. H. Edwards, *Neuron* **2010**, *65*, 66–79; c) M. J. Farrer, *Nat. Rev. Genet.* **2006**, *7*, 306–318.

[3] a) M. Drescher, M. Huber, V. Subramaniam, *ChemBioChem* **2012**, *13*, 761–768; b) M. E. van Raaij, J. van Gestel, I. M. J. Segers-Nolten, S. W. de Leeuw, V. Subramaniam, *Biophys. J.* **2008**, *95*, 4871–4878; c) W. Hoyer, T. Antony, D. Cherny, G. Heim, T. M. Jovin, V. Subramaniam, *J. Mol. Biol.* **2002**, *322*, 383–393; d) L. A. Munishkina, J. Henriques, V. N. Uversky, A. L. Fink, *Biochemistry* **2004**, *43*, 3289–3300.

[4] P. K. Auluck, G. Caraveo, S. Lindquist, *Annu. Rev. Cell Dev. Biol.* **2010**, *26*, 211–233.

[5] a) R. Bussell, T. F. Ramlall, D. Eliezer, *Protein Sci.* **2005**, *14*, 862–872; b) K. K. Dev, H. van der Putten, B. Sommer, G. Rovelli, *Neuropharmacology* **2003**, *45*, 1–13.

[6] a) M. Robotta, P. Braun, B. van Rooijen, V. Subramaniam, M. Huber, M. Drescher, *ChemPhysChem* **2011**, *12*, 267–269; b) W. S. Davidson, A. Jonas, D. F. Clayton, J. M. George, *J. Biol. Chem.* **1998**, *273*, 9443–9449; c) I. Dikiy, D. Eliezer, *Biochim. Biophys. Acta Biomembr.* **2012**, *1818*, 1013–1018.

[7] W. P. Gai, H. X. Yuan, X. Q. Li, J. T. H. Power, P. C. Blumbergs, P. H. Jensen, *Exp. Neurol.* **2000**, *166*, 324–333.

[8] H. Y. Kim, M. K. Cho, A. Kumar, E. Maier, C. Siebenhaar, S. Becker, C. O. Fernandez, H. A. Lashuel, R. Benz, A. Lange, M. Zweckstetter, *J. Am. Chem. Soc.* **2009**, *131*, 17482–17489.

[9] a) T. Doussineau, C. Mathevon, L. Altamura, C. Vendrely, P. Dugourd, V. Forge, R. Antoine, *Angew. Chem. Int. Ed.* **2016**, *55*, 2340; *Angew. Chem.* **2016**, *128*, 2386; b) R. Mishra, B. Bulic, D. Sellin, S. Jha, H. Waldmann, R. Winter, *Angew. Chem. Int. Ed.* **2008**, *47*, 4679–4682; *Angew. Chem.* **2008**, *120*, 4757–4760; c) R. Sarroukh, E. Goormaghtigh, J. M. Ruysschaert, V. Raussens, *Biochim. Biophys. Acta Biomembr.* **2013**, *1828*, 2328–2338; d) G. Zandomeneghi, M. R. H. Krebs, M. G. McCammon, M. Fändrich, *Protein Sci.* **2004**, *13*, 3314–3321.

[10] a) K. Hauser, C. Krejtschi, R. Huang, L. Wu, T. A. Keiderling, *J. Am. Chem. Soc.* **2008**, *130*, 2984–2992; b) A. W. Smith, A. Tokmakoff, *Angew. Chem. Int. Ed.* **2007**, *46*, 7984–7987; *Angew. Chem.* **2007**, *119*, 8130–8133; c) M. A. Fallah, C. Stanglmair, C. Pacholski, K. Hauser, *Langmuir* **2016**, *32*, 7356–7364; d) K. Henke, W. Welte, K. Hauser, *Biochemistry* **2016**, *55*, 4333–4343.

[11] a) M. Jackson, H. H. Mantsch, *Crit. Rev. Biochem. Mol. Biol.* **1995**, *30*, 95–120; b) A. Barth, C. Zscherp, *Q. Rev. Biophys.* **2002**, *35*, 369–430.

[12] a) R. J. Perrin, W. S. Woods, D. F. Clayton, J. M. George, *J. Biol. Chem.* **2000**, *275*, 34393–34398; b) K. Beyer, *Acta Neuropathol.* **2006**, *112*, 237–251; c) K. Ueda, T. Saitoh, H. Mori, *Biochem. Biophys. Res. Commun.* **1994**, *205*, 1366–1372.

[13] D. Eliezer, E. Kutluay, R. Bussell, G. Browne, *J. Mol. Biol.* **2001**, *307*, 1061–1073.

[14] a) K. A. Conway, J. D. Harper, P. T. Lansbury, Jr., *Biochemistry* **2000**, *39*, 2552–2563; b) L. Giehm, D. I. Svergun, D. E. Otzen, B. Vestergaard, *Proc. Natl. Acad. Sci. USA* **2011**, *108*, 3246–3251; c) M. S. Celej, R. Sarroukh, E.

Goormaghtigh, G. D. Fidelio, J. M. Ruysschaert, V. Raussens, *Biochem. J.* **2012**, *443*, 719 – 726.

[15] a) P. Pinkerneil, J. Guldenhaupt, K. Gerwert, C. Kötting, *ChemPhysChem* **2012**, *13*, 2649 – 2653; b) C. Kötting, J. Guldenhaupt, K. Gerwert, *Chem. Phys.* **2012**, *396*, 72 – 83.

[16] a) Y. Tashima, R. Oe, S. Lee, G. Sugihara, E. J. Chambers, M. Takahashi, T. Yamada, *J. Biol. Chem.* **2004**, *279*, 17587 – 17595; b) T. Hoshino, M. I. Mahmood, K. Mori, K. Matsuzaki, *J. Phys. Chem. B* **2013**, *117*, 8085 – 8094; c) K. Sasahara, K. Morigaki, K. Shinya, *Phys. Chem. Chem. Phys.* **2013**, *15*, 8929 – 8939; d) M. Calamai, F. S. Pavone, *FEBS Lett.* **2013**, *587*, 1385 – 1391; e) C. L. Schengrund, *Brain Res. Bull.* **2010**, *82*, 7 – 17.

[17] a) Z. Martinez, M. Zhu, S. B. Han, A. L. Fink, *Biochemistry* **2007**, *46*, 1868 – 1877; b) C. Di Scala, N. Yahi, S. Boutemeur, A. Flores, L. Rodriguez, H. Chahinian, J. Fantini, *Sci. Rep.* **2016**, *6*, 28781.

[18] a) T. S. Ulmer, A. Bax, N. B. Cole, R. L. Nussbaum, *J. Biol. Chem.* **2005**, *280*, 9595 – 9603; b) M. Drescher, G. Veldhuis, B. D. van Rooijen, S. Milikisyants, V. Subramaniam, M. Huber, *J. Am. Chem. Soc.* **2008**, *130*, 7796 – 7797; c) C. C. Jao, B. G. Hegde, J. Chen, I. S. Haworth, R. Langen, *Proc. Natl. Acad. Sci. USA* **2008**, *105*, 19666 – 19671; d) M. Robotta, H. R. Gerding, A. Vogel, K. Hauser, S. Schildknecht, C. Karreman, M. Leist, V. Subramaniam, M. Drescher, *ChemBioChem* **2014**, *15*, 2499 – 2502.

[19] a) N. P. Reynolds, A. Soragni, M. Rabe, D. Verdes, E. Liverani, S. Handschin, R. Riek, S. Seeger, *J. Am. Chem. Soc.* **2011**, *133*, 19366 – 19375; b) M. M. Ouberai, J. Wang, M. J. Swann, C. Galvagnion, T. Guilliams, C. M. Dobson, M. E. Welland, *J. Biol. Chem.* **2013**, *288*, 20883 – 20895; c) A. Iyer, N. O. Petersen, M. M. A. E. Claessens, V. Subramaniam, *Biophys. J.* **2014**, *106*, 2585 – 2594.